Hyperthermal Ar atom scattering from a C(0001) surface

K. D. Gibson,[1] S. J. Sibener,[1,a)] Hari P. Upadhyaya,[2] Amy L. Brunsvold,[2] Jianming Zhang,[2] Timothy K. Minton,[2] and Diego Troya[3]
[1]*The James Franck Institute and Department of Chemistry, The University of Chicago, 929 E. 57th Street, Chicago, Illinois 60637, USA*
[2]*Department of Chemistry and Biochemistry, Montana State University, Bozeman, Montana 59717, USA*
[3]*Department of Chemistry, Virginia Tech, 107 Davidson Hall, Blacksburg, Virginia 24061, USA*

(Received 21 February 2008; accepted 17 April 2008; published online 13 June 2008)

Experiments and simulations on the scattering of hyperthermal Ar from a C(0001) surface have been conducted. Measurements of the energy and angular distributions of the scattered Ar flux were made over a range of incident angles, incident energies (2.8–14.1 eV), and surface temperatures (150–700 K). In all cases, the scattering is concentrated in a narrow superspecular peak, with significant energy exchange with the surface. The simulations closely reproduce the experimental observations. Unlike recent experiments on hyperthermal Xe scattering from graphite [Watanabe *et al.*, Eur. Phys. J. D **38**, 103 (2006)], the angular dependence of the energy loss is not approximated by the hard cubes model. The simulations are used to investigate why parallel momentum conservation describes Xe scattering, but not Ar scattering, from the surface of graphite. These studies extend our knowledge of gas-surface collisional energy transfer in the hyperthermal regime, and also demonstrate the importance of performing realistic numerical simulations for modeling such encounters. © *2008 American Institute of Physics*. [DOI: 10.1063/1.2924126]

INTRODUCTION

The scattering of gases from surfaces has a long history, helping to elucidate the microscopic details of such processes as reactivity, sputtering, and the aerodynamic drag of an object moving through the atmosphere.[1] Rare gases are useful in that they are nonreactive and have only a relatively weak attractive interaction, making it possible to isolate the collisional dynamics to hard-sphere-like interactions. In this paper, we present the results of experimental and theoretical studies of the angle- and energy-resolved scattering of hyperthermal Ar (translational energies of 2.8–14.1 eV) from the surface of an ordered highly oriented pyrolytic graphite (HOPG) surface. This system has a few particularly interesting features. The projectile is more than three times the mass of a surface atom. Most previous studies of scattering from ordered surfaces have involved heavier substrates, and usually the impinging gas atom was lighter. Ar+HOPG also serves as a model for understanding the hyperthermal scattering of closed-shell molecules, such as N_2, with the surface of spacecraft in low Earth orbit (LEO, 200–700 km altitude).

The surface of HOPG is only slightly corrugated,[2] so we will briefly consider previous experiments that have examined the scattering of rare gases (translational energies of $<1-14$ eV) from other flat surfaces or along the uncorrugated azimuthal direction of corrugated surfaces. These include Xe–Ni(111),[3] Xe–Pt(111),[4,5] Xe–GaAs(100),[6] Xe–Ag(100),[6] Xe–Ge(100),[6] Ar–Pt(111),[5] Ar–Ag(111),[7] and Ar–Ru(0001).[8] For incident energies greater than about 1 eV, the angular distribution of the scattered flux is concentrated in one peak whose intensity maximum is at the specular or larger angle. In general, this distribution is fairly narrow, at least for the lowest surface temperatures, with a full-width half-maximum (FWHM) of $\sim 10°-20°$.

The scattering of atoms from surfaces may be divided into two regimes.[9] At the lowest incident velocities, the atom has time to interact with many of the surface atoms as it approaches. In this so-called thermal regime, the scattering can sometimes be described with the simplest hard cubes model,[9] which predicts parallel momentum conservation (PMC), $E_F/E_I=(\sin\Theta_I/\sin\Theta_F)^2$, where E_I and E_F are the initial and final translational energies of the Ar, respectively, and Θ_I and Θ_F are the pre- and postcollision angles with respect to the surface normal, respectively. A salient feature of this type of scattering is that the energy of the scattered atoms decreases as the angle at which they are scattered increases. There is a further refinement of the hard cubes model when the surface appears corrugated to the impinging atom.[10] In this case, there is PMC with the tangent to the surface at the point of impact, leading to a nonmonotonic structure in the energy of the scattered atoms as a function of scattering angle. PMC also often leads to a rainbow structure in the angular intensity distribution. This structure may be unresolved as a result of the thermal motion of the surface, although there would still probably be a broad and asymmetric angular intensity distribution. The Ar–Ru(0001) data[8] exhibit this behavior in the angular energy distribution although probably not in the angular intensity distribution, even though one would not expect the surface to appear corrugated. As the velocity of the incoming atom increases, the interaction involves one or a few surface atoms: the structure scattering regime. Here, one possible description is a simple binary model assuming one or more collisions between

a)Author to whom correspondence should be addressed. Electronic mail: s-sibener@uchicago.edu.

spheres.[6,11] This leads to an increase in the energy of the scattered atoms with increasing scattering angle, opposite to the hard cubes behavior.

An instructive experiment was done by Rettner *et al.*,[4] where the relationship between scattering angle and final energy of Xe scattering from Pt(111) was monitored as a function of the Xe incident energy. At the lowest E_I (0.5 eV), the measured values of E_F came close to the predictions of PMC. As the incident energy was increased through stages up to 14.3 eV, the angular dependence of the final energy clearly changed; the final energy increased with increasing scattering angle.

Recently, an experiment involving the scattering of hyperthermal Xe from graphite was reported.[12,13] For incident energies from ~0.5 to 3.5 eV, the scattering behavior was well reproduced by the simple hard cubes model with PMC. Here we report experimental and theoretical studies of the scattering of Ar from a similar surface. These studies, which employ a smaller projectile mass and an overlapping range of energies, reveal details in the scattering dynamics that were not uncovered by the earlier study on Xe scattering from graphite.

EXPERIMENTAL DETAILS

Scattering experiments were done at both the University of Chicago and Montana State University (MSU). At the University of Chicago, scattering occurs in an ultrahigh vacuum (UHV) chamber with a base pressure of 1×10^{-10} Torr. The sample is mounted on a rotating manipulator so that the incident polar angle (Θ_I) can be varied. The sample can also be resistively heated and cryogenically cooled with liquid N_2. There is a separately rotating, double-differentially pumped quadrupole mass spectrometer (QMS) (~1° FWHM angular resolution) to detect the scattered Ar atoms. The experimental technique used at MSU is similar, employing a crossed molecular beam apparatus configured for studies of gas-surface interactions.[14,15] A pulsed beam containing hyperthermal Ar atoms was directed at the surface, and a rotatable UHV mass spectrometer detector was used to monitor scattered Ar atoms that scattered from a resistively heated target surface. The electron bombardment ionizer of the detector is 33.7 cm from the surface, and the acceptance angle of the detector is ~2°. The surface and detector rotate about the same axis, with the surface normal rotating in the same plane as the detector. The base pressure of the main scattering chamber is 10^{-7} Torr (pumped with cryopumps and a large liquid-nitrogen-cooled panel). In experiments on both apparatuses, inelastically scattered Ar atoms were measured as a function of incident angle Θ_I and final angle Θ_F with respect to the surface normal. For characterization of the incident beam, the surface was lowered out of the beam path, and the beam was directed into the detector.

At both laboratories, the hyperthermal translational energy Ar atoms were produced with a laser-breakdown source originally developed by Physical Sciences, Inc.[16] and further refined by the Minton group.[14] A pulse of Ar is produced from a piezoelectric pulsed valve inspired by the Proch and Trickl design.[17] The Ar expands into a gold-plated Cu cone. After a delay of 200–300 μs, a pulsed CO_2 laser is fired and the light is focused into the narrow end of the cone with a spherical mirror (1 m radius of curvature), where it induces a breakdown and rapidly heats the gas to more than 20 000 K. The hot gas expands from a confined region of space, making the laser-breakdown source effectively a point source. However, the gas pulse that exits the conical nozzle has a fairly broad velocity distribution. Therefore, a single synchronized chopper wheel (slotted disk) is used to select a portion of the initial velocity profile. The chopper wheel blocks all of the light emitted by the source plasma and essentially all the residual ions, which travel at higher velocities than most of the atoms in the neutral beam pulse. The velocity distributions of the hyperthermal Ar are determined by time-of-flight (TOF) spectroscopy, using a multichannel scaler system. The TOF distributions, which are number density distributions as a function of arrival time at the ionizer of the detector $N(t)$, may be transformed into translational energy distributions, yielding probability density distributions as a function of energy $P(E_T)$. One incident beam was used for experiments at MSU, with an average translational energy $\langle E_I \rangle$ of 8.3 eV. Three beams were used at the University of Chicago, with $\langle E_I \rangle$=2.8, 8.5, and 14.1 eV. The translational energy distributions are shown in Fig. 1.

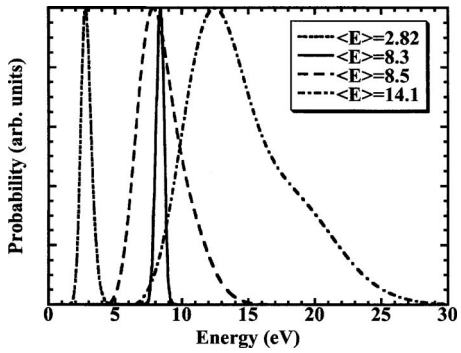

FIG. 1. Energy distributions for the Ar beam energies. The peak intensities have been adjusted to have the same value for comparison purposes.

In all experiments, a HOPG sample was mounted on a manipulator after exposing a fresh surface by removing the upper layers with tape. In the Chicago experiment, after mounting the sample (SPI-Materials, ZYA grade), the UHV chamber was then evacuated and baked at ~425 K to reach the final pressure of 1×10^{-10} Torr. Finally, the graphite surface was annealed for a few days at 700 K.[2] This annealing could be monitored by either fast Ar or low energy specular He scattering. For both methods, the peak intensity increased and the width of the scattered angular intensity distribution decreased until the surface was completely annealed. He diffraction spectra showed a narrow specular and higher order diffraction features, demonstrating that the surface was flat and well-ordered. Scattering data were collected with different sample temperatures. At MSU, the sample (ZYA quality, Advanced Ceramics, formerly known as Union Carbide) was first heated under vacuum at 540 K for ~60 h to remove contamination and anneal the surface. The sample temperature was reduced somewhat (508 K) for data collection. A

series of Ar scattering experiments were conducted at MSU with sample temperatures from 300 to 560 K, and it was found that the scattering dynamics no longer changed at temperatures of 480 K and above. Furthermore, the scattering dynamics remained unchanged when the sample was held indefinitely at these high temperatures. Therefore, the sample was assumed to be free from contamination for the data collected at 508 K, which are reported here.

SCATTERING SIMULATIONS

We have simulated the collisions of Ar with graphite using classical trajectories. The trajectories have been integrated using a hybrid potential-energy surface, which considers separate terms for the gas/surface and surface potential. The second-generation reactive empirical bond order potential by Brenner *et al.*[18] has been used to simulate the graphite potential during the collisions. The Ar/graphite interactions have been modeled using a pairwise potential, which we have derived based on *ab initio* calculations. The *ab initio* calculations consider three approaches of Ar to reduced-dimensionality graphite mimics. In the first approach, we have calculated the potential of Ar attacking the benzene molecule in a line perpendicular to the benzene plane that passes through the center of mass of the molecule. In the second approach, we have mapped the potential for Ar striking a naphthalene molecule along a line perpendicular to the naphthalene molecule that passes through the middle of the central C–C bond of the molecule. The third approach is similar to the second but the line defining the approach of Ar to naphthalene passes through one of the C atoms of the central C–C bond. Overall, 142 points were calculated at the MP2/aug-cc-pVTZ level, covering regions of the potential-energy surface from the asymptote up to repulsions of about 14 eV along these three approaches. Using these *ab initio* energies, we have derived analytical pairwise Buckingham potentials. The potential for each Ar–C pair is of the following form:

$$V_{\mathrm{Ar-C}} = A\,\exp^{(-B*r_{\mathrm{Ar-C}})} + \frac{C}{r_{\mathrm{Ar-C}}{}^{6}} + \frac{D}{r_{\mathrm{Ar-C}}{}^{9}} + \frac{E}{r_{\mathrm{Ar-C}}{}^{12}}, \qquad (1)$$

where

$A = 112\,731.644$ kcal/mol,

$B = 3.630\,284\,61$ Å^{-1},

$C = 183.757\,572$ kcal mol^{-1} Å^{6},

$D = -20\,408.3304$ kcal mol^{-1} Å^{9},

and

$E = 23\,741.3606$ kcal mol^{-1} Å^{12}.

In order to make contact with experiment, we have calculated 1000 trajectories for each set of incident angle and collision energy explored in the experiment. The surface initial coordinates and momenta were obtained from a canonical molecular-dynamics simulation at either 150 or 508 K, to compare with the experiments at Chicago and MSU, respectively. The model of graphite used in the simulations consists of 280 atoms of C distributed in two layers of 17.2 $\times$21.3 Å^2 area. Sample simulations with additional layers (a total of three and four layers) gave identical results to the ones calculated with two layers. Trajectories were started at an initial distance of 10 Å between Ar and the nearest atom on the graphite surface and were stopped when the distance between the recoiling Ar and the closest atom on the surface was at least 10 Å after collision. The integration time step was set to 25 a.u. (0.6 fs).

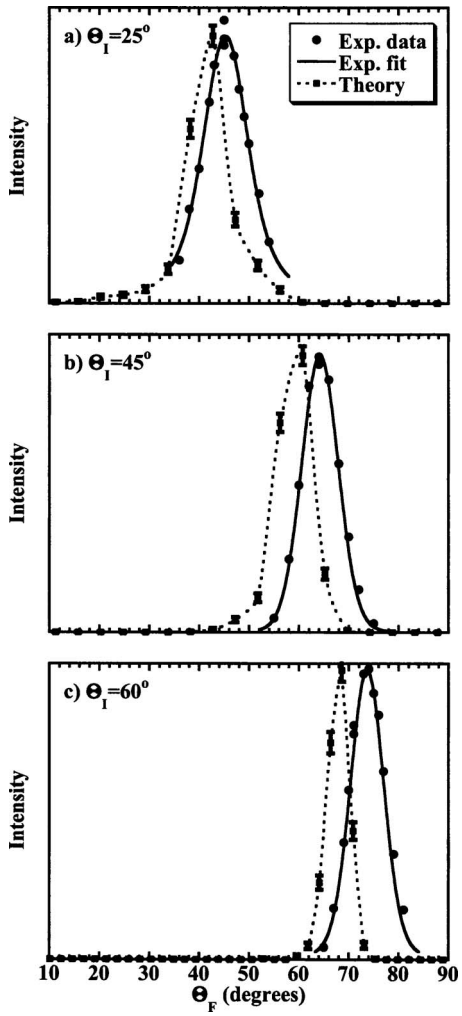

FIG. 2. Plots of the scattering intensity for an incident Ar average kinetic energy of 2.8 eV and T_S=150 K. The filled circles are the experimental data points, the line through them is a fit to the data, the squares are the theory calculations with error bars superimposed, and the dotted line is an interpolation between these points.

RESULTS

Figures 2–5 show the in-plane angular intensity distributions, the total intensity of the Ar scattered at the indicated Θ_I and Θ_F, and average final translational energies for some of the measurements at different incident angles, incident energies, and different surface temperatures. Figures 2 and 3 show University of Chicago data where T_S=150 K and the average energy of the incident Ar was 2.8 eV. Figures 4 and 5 show MSU data where T_S=508 K and the average energy of the incident Ar was 8.3 eV. The filled circles are derived

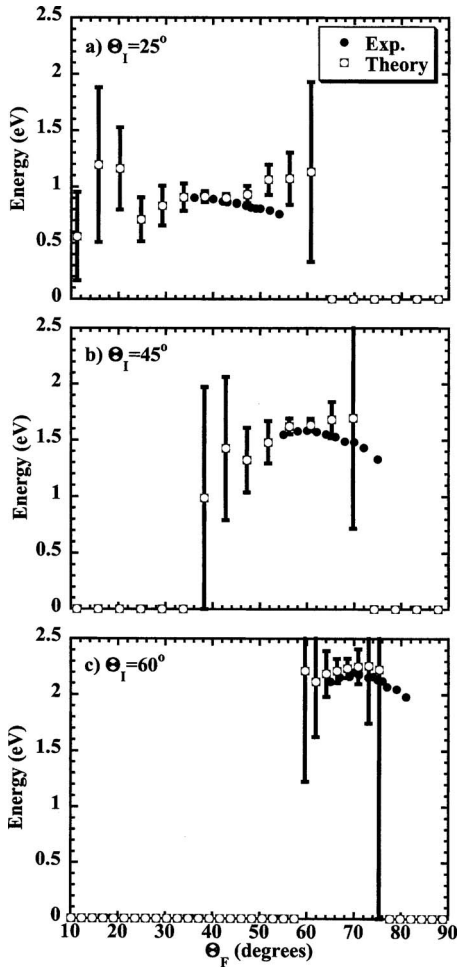

FIG. 3. Plots of the average energy of the scattered Ar for an incident average kinetic energy of 2.8 eV and T_S=150 K. The filled circles are the experimental data points and the squares are the theory calculations with error bars superimposed.

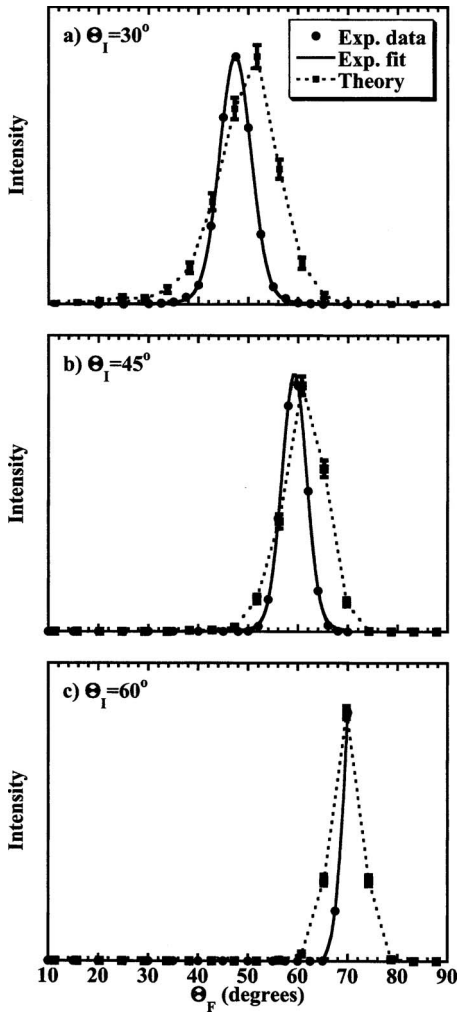

FIG. 4. Same as Fig. 2, but for an average kinetic energy of 8.3 eV and T_S=508 K.

from experimental scattering data, and the squares depict the results of the trajectory calculations. Figures summarizing experiments performed at other conditions are included as additional material.[19] Together, all of the data sets provide broad coverage of the scattering behavior. The in-plane scattering intensity is concentrated in a narrow superspecular peak. The angular position of the maximum scattering intensity is dependent on the angle of incidence, but it is only slightly dependent on the incident Ar translational energy from 2.8 to 14.1 eV. All scattering appears to be direct; none of the data showed any measurable signal compatible with trapping-desorption, where the energy of the scattered Ar would be $2kT_S$. Although no signal was detected at final angles much lower than the peak in the angular distributions collected at the University of Chicago, very small signals (less than one percent of the peak) were detected in the MSU data at angles all the way down to a final angle of 0°. These tiny signals might be the result of imperfect annealing of the surface or residual contamination, or they may simply reflect the difference in sensitivities of the two experiments. In any case, the experimental results in both laboratories show very similar scattering behavior, and the theoretical calculations were not sensitive to improbable scattering events that lead to Ar exiting the surface at small angles.

The simulations show good agreement with the experimental data. The differences between the peaks of the calculated and experimental distributions are less than 5° in all cases. The calculated average energy of the scattered Ar is quite close to the experimental average energy in the region of the peak of the angular distributions. Considering that the calculations are for a single incident energy, whereas the experimental incident energies are rather broad the agreement is quite good. It should also be noted that the calculated results in Figs. 2–5 consider all trajectories, including those that do not show in-plane scattering. Nevertheless, out-of-plane scattering is a very small fraction of the total flux in the calculations (more than 85% of the trajectories scatter within ±10° of the in-plane direction).

DISCUSSION

As mentioned in the introduction, a recent study reported the dynamical behavior of hyperthermal Xe (incident energies up to 3.6 eV) scattering from HOPG.[12] These researchers determined that a simple hard cubes model, where the surface is flat and parallel momentum is conserved, with a cube mass m_{surface} of ~300 amu described the data well. However, for Ar scattering, even at 2.8 eV, PMC does not

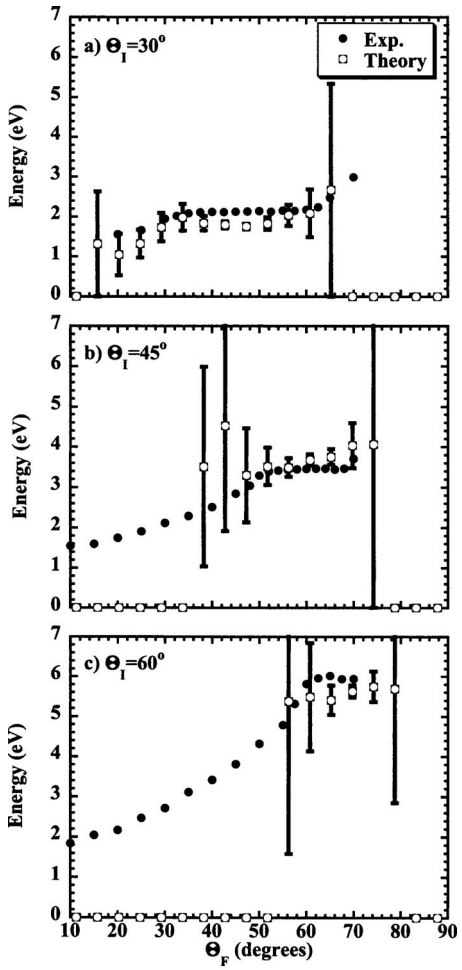

FIG. 5. Same as Fig. 3, but for an incident average kinetic energy of 8.3 eV and T_S=508 K.

come close to describing the data. At the scattering angles where appreciable Ar flux is observed, the final energies are much less than what would be predicted with PMC. Instead, a binary collision model without PMC describes the data (see Fig. 6). In this model,[11]

$$\frac{E_F}{E_I} = \left(\frac{\sqrt{1-\mu^2 \sin^2 \Theta_T} - \mu \cos \Theta_T}{1+\mu} \right)^2, \tag{2}$$

where $\mu = m_{\mathrm{Ar}}/m_{\mathrm{surface}}$ and $\Theta_T = \Theta_I + \Theta_F$. The value of m_{surface}=70–100 amu, which is considerably less than the average cube mass derived from the experiment on Xe scattering from HOPG.[12] The inverse relationship between m_{surface} and the velocity of the impinging gas atom is what is qualitatively expected,[20] but it is unclear what m_{surface} physically represents.[21] The binary collision model is a simple two-dimensional model that is strictly valid for the single collision between two spheres, but it is apparent from the value of μ that more than one surface atom is involved. As will be discussed below, there is also a problem in ignoring the attractive part of the gas-surface interaction potential in the incident energy range of a few eV for some systems. These models, though they can be used to describe the data, do not fully elucidate the underlying physics.

To shed light on the Ar/graphite collision mechanism, we have investigated how many collisions take place between

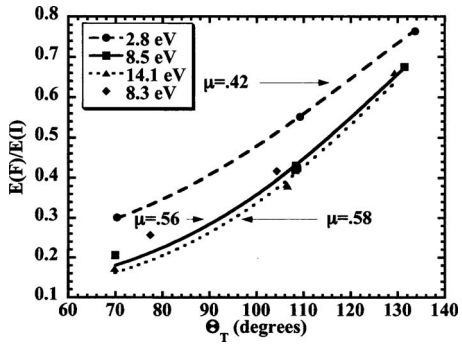

FIG. 6. Plots of E_F/E_I vs $\Theta_T = \Theta_I + \Theta_F$ for all of the data. The values of Θ_F and E_F are from the maxima of the intensity distributions. The lines correspond to the binary collision model with the indicated value of $\mu = m_{\mathrm{Ar}}/m_{\mathrm{surface}}$.

the impinging atom and the surface at the initial conditions of this study. Operationally, we have achieved this by monitoring the behavior of the Ar atom coordinate along the surface-normal axis in each trajectory. Our analysis reveals that all of the trajectories involve only one collision between the Ar atom and the surface, i.e., there is only one minimum in the coordinate of the Ar atom along the surface-normal axis in each trajectory, though the Ar interacts with several surface atoms during this one collision. As examples, animations of trajectory calculations for the collision of 14.1 eV Ar at Θ_I=30° are attached.[19] This result is expected due to the small attraction between the Ar atom and the surface, which is not large enough to overcome the kinetic energy retained by the Ar atom after collision. Quantitatively, our MP2/aug-cc-pVTZ *ab initio* calculations of the interaction potential between Ar and reduced-dimensionality models of graphite show well depths well below 3 kcal mol^{-1} in all cases. In fact, the deepest well of the three approaches of Ar to benzene or naphthalene explored in this work occurs for the approach of Ar perpendicular to the central bond in the naphthalene molecule. At the MP2/aug-cc-pVTZ level, and including basis-set superposition error via the counterpoise method, the well depth is 1.96 kcal mol^{-1} at a distance of 3.4 Å between the Ar atom and the center of the central bond in naphthalene. This energy is to be compared with the average experimentally determined final energy of the recoiling Ar atom. The lowest final energy of Ar measured in the experiment, ~0.5 eV or 11.5 kcal mol^{-1}, occurs when Ar recoils in a direction near-parallel to the surface normal after colliding with the surface at 2.8 eV and a 25° incidence angle (Fig. 3). This lowest recoil energy is still more than five times larger than the most attractive part of the potential, thereby explaining the fact that the trajectories only exhibit one collision between Ar and the surface. Sample calculations using Ar-graphite analytic intermolecular potentials that were artificially more attractive than predicted by *ab initio* calculations exhibited a few trajectories with more than one Ar/graphite collision. Nevertheless, the number of trajectories undergoing this behavior was less than 5% of the total.

To further investigate the origin of the apparent agreement between the measurements of Xe scattering from graphite and the predictions of the hard cubes model, we have carried out trajectory calculations of Xe colliding with

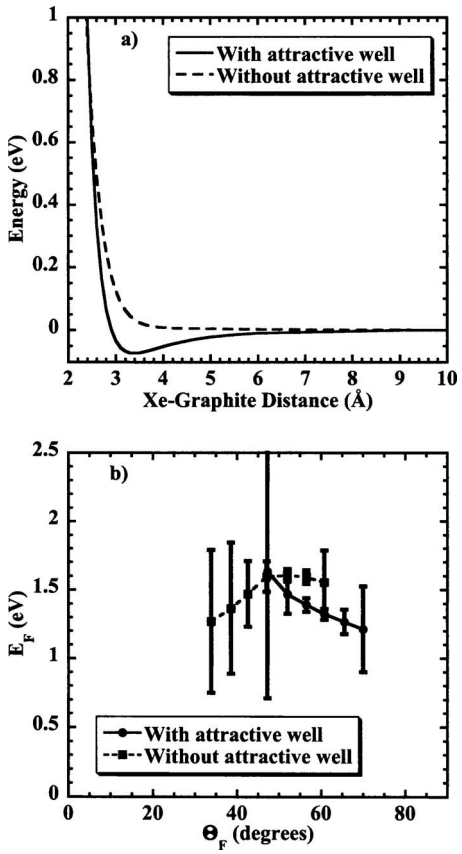

FIG. 7. (a) Potential-energy profile of the Xe-graphite intermolecular potentials used in this work along a perpendicular approach of Xe to a model graphite surface. (b) Average Xe final energy as a function of the polar scattering angle at E_I=3.62 eV and 35° incidence angle.

graphite at 3.62 eV and with a 35° incidence angle with two different gas/surface potentials. First, we have used the Xe-graphite pairwise potential used by Watanabe *et al.*[12] This intermolecular potential possesses an attractive well. Second, we have used a Xe-graphite potential that is purely repulsive. A comparison of the potential energy curves provided by both analytic functions is plotted in Fig. 7(a). These potential-energy curves correspond to an approach of Xe perpendicular to the graphite slab used in the trajectory calculations. Figure 7(b) shows the average final energy of the recoiling Xe atom as a function of the final scattering angle for both potential-energy surfaces. The calculations using the attractive potential match those of Watanabe and experiment, whereas those using the purely repulsive potential do not. Interestingly, the calculations that consider a potential-energy surface containing attraction between Xe and graphite also agree with the predictions of the hard cubes model (the recoil energy decreases with final angle), but the calculations that use the purely repulsive potential do not. This result seems counterintuitive, because the hard cubes model assumes that there is no attraction between the gas and the surface. It therefore seems that the ability of the hard cubes model to reproduce experiments and detailed trajectory calculations of Xe scattering from graphite that consider an attractive potential is fortuitous.

A second point of interest in the comparison of the results including or not an attractive term in the gas/surface potential is the apparent shift in the angular intensity that can be inferred from Fig. 7(b). In effect, the calculations that consider an attractive potential yield angular distributions that are shifted to larger final angles than the ones obtained with a purely repulsive potential. An intuitive explanation for this result is that the attractive part of the potential influences the postcollision pathway of Xe by decreasing the recoil speed component along the axis perpendicular to the surface. This causes an increase in the final scattering angle in comparison with the results of a potential that does not have an attractive term.

The important point of these calculations is that the apparent agreement between the Xe-HOPG scattering results and the PMC predictions appears to be fortuitous. Agreement is dependent on the strength of the Xe-graphite interaction potential, which is not considered in a simple parallel momentum conservation model.

CONCLUSIONS

This paper presents the results of both experiments and simulations of the scattering of hyperthermal Ar from an ordered HOPG surface. For all of the incident angles, incident energies (2.8–14.1 eV), and surface temperatures (150–700 K), the in-plane scattered Ar atoms were concentrated in a narrow superspecular range after significant energy loss to the surface. The simulations matched these results well. Of particular interest was the comparison with an earlier study that probed hyperthermal Xe scattering from the same surface.[12,13] For the entire range of Xe energies (0.5–3.6 eV), the scattering could be reproduced using a simple hard cubes model with a surface mass of ~300 amu. For Ar, the energy exchange with the surface was much larger than predicted by a hard cubes model: The predicted value of E_F was as much as a factor of 2 greater than that measured at the final angles where scattering is observed. Overall, the angular dependence of the energy appeared to be in the structure scattering regime, where the interaction involves only one or a few surface atoms. In fact, a simple binary model, derived using the assumption of a single collision between two spheres, does approximately represent the data.

The simulations that were performed for hyperthermal Xe scattering from an HOPG surface revealed that the apparently good agreement with the hard cubes model was fortuitous and resulted from the attractive part of the potential, which the hard cubes model ignores. Although simple models often capture the essential physics, they can, as shown in our results, sometimes lead to erroneous conclusions. It is therefore advantageous to utilize detailed dynamics simulations in combination with the ever increasing availability of fast and cheap computational power.

These studies add to our knowledge of gas-surface collisional energy transfer in the hyperthermal regime, and they also demonstrate the importance of performing realistic numerical simulations for modeling such encounters. This regime is not only of fundamental interest but is of direct rel-

evance to understanding both momentum and energy exchange between space vehicles and the ambient atmosphere.

ACKNOWLEDGMENTS

One of the authors (S.J.S.) acknowledges support from the Air Force Office of Scientific Research through Grant No. FA9550-06-1-0139 and the NSF-MRSEC at the University of Chicago, Grant No. NSF-DMR-0213745. Another author (T.K.M.) acknowledges support from the AFOSR through Grant No. FA9550-04-1-0428. Another author (D.T.) acknowledges funding from AFOSR Grant. No FA9550-06-1-0165 and NSF Grant No. 0547543. One of the authors (D.T.) is a Cottrell Scholar of Research Corporation.

[1] T. K. Minton, M. Tagawa, and G. M. Nathanson, J. Spacecr. Rockets **41**, 389 (2004).
[2] G. Boato, P. Cantini, and R. Tatarek, Phys. Rev. Lett. **40**, 887 (1978).
[3] M. Ellison, C. M. Matthews, and R. N. Zare, J. Chem. Phys. **112**, 1975 (2000).
[4] C. T. Rettner, J. A. Barker, and D. S. Bethune, Phys. Rev. Lett. **67**, 2183 (1991).
[5] H. F. Winters, H. Coufal, C. T. Rettner, and D. S. Bethune, Phys. Rev. B **41**, 6240 (1990).
[6] A. Amirav, M. J. Cardillo, P. L. Trevor, C. Lim, and J. C. Tully, J. Chem. Phys. **87**, 1796 (1987).
[7] A. Raukema, R. J. Dirksen, and A. W. Kleyn, J. Chem. Phys. **103**, 6217 (1995).
[8] B. Berenbak, S. Zboray, B. Riedmuller, D. C. Papageorgopoulos, S. Stolte, and A. W. Kleyn, Phys. Chem. Chem. Phys. **4**, 68 (2002).
[9] F. O. Goodman and H. Y. Wachman, *Dynamics of Gas-Surface Scattering* (Academic, New York, 1976).
[10] J. C. Tully, J. Chem. Phys. **92**, 680 (1990).
[11] R. J. W. E. Lahaye and H. Kang, Surf. Sci. **490**, 327 (2001).
[12] Y. Watanabe, H. Yamaguchi, M. Hashinokuchi, K. Sawabe, S. Maruyama, Y. Matsumoto, and K. Shobatake, Eur. Phys. J. D **38**, 103 (2006).
[13] Y. Watanabe, H. Yamaguchi, M. Hashinokuchi, K. Sawabe, S. Maruyama, Y. Matsumoto, and K. Shobatake, Chem. Phys. Lett. **413**, 331 (2005).
[14] J. Zhang, D. J. Garton, and T. K. Minton, J. Chem. Phys. **117**, 6239 (2002).
[15] J. Zhang, H. P. Upadyaya, A. L. Brunsvold, and T. K. Minton, J. Phys. Chem. B **110**, 12500 (2006).
[16] G. E. Caledonia, R. H. Krech, and D. B. Green, AIAA J. **25**, 59 (1987).
[17] D. Proch and T. Trickl, Rev. Sci. Instrum. **60**, 713 (1988).
[18] D. W. Brenner, O. A. Shenderova, J. A. Harrison, S. J. Stuart, B. Ni, and S. B. Sinnott, J. Phys.: Condens. Matter **14**, 783 (2002).
[19] See EPAPS Document No. E-JCPSA6-128-022821 for Additional.pdf, Trajectory1.avi, and Trajectory 2.avi. For more information on EPAPS, see http://www.aip.org/pubservs/epaps.html.
[20] D. Velic and R. J. Levis, Chem. Phys. Lett. **269**, 59 (1997).
[21] V. K. Ferleger and I. A. Wojciechowski, Nucl. Instrum. Methods Phys. Res. B **164–165**, 641 (2000).